Hindawi
Mathematical Problems in Engineering
Volume 2020, Article ID 4802930, 9 pages
https://doi.org/10.1155/2020/4802930

Research Article

Dispersion of an SH-Guided Wave in Weld Seam Based on Peridynamics Theory

Xiaolong Zhang and Zhenying Xu

School of Mechanical Engineering, Jiangsu University, Zhenjiang 212013, China

Correspondence should be addressed to Zhenying Xu; zhyxu77@163.com

Received 18 October 2019; Revised 19 December 2019; Accepted 10 January 2020; Published 31 January 2020

Academic Editor: Alessandro De Luca

The dispersion characteristics of shear horizontal- (SH-) guided waves in a weld seam are critical to identifying defects. By considering the force on the virtual boundary layer near the weld surface, a dispersion equation for the SH-guided wave in the weld seam was established here based on the peridynamics method. The wave dispersion equation is similar to the traditional theory. The SH wave in the infinite peridynamics medium has dispersion characteristics, and the group velocity of the SH-guided wave in the weld seam is slightly slower than that in the conventional theory. In the welded structure, the group velocity of the SH-guided wave is unevenly distributed in different regions due to the differences in material parameters between the weld seam and the steel plate and residual weld height on the weld seam. The distance from the different sensors to the defect can be precisely calculated via the group velocity distribution; thus, the defect can be accurately located. By compared with the finite element method and experiments under the same conditions, the reliability of the peridynamics method is verified. We used the group velocity of the SH-guided wave in the weld seam and peridynamics theory to better reflect the experimental conditions versus finite element simulations.

1. Introduction

Welding is critical in steel structures, and welding quality directly affects the safety of the entire structure [1–5]. Therefore, detection of weld seams is particularly important. Weld inspection methods include magnetic powder methods [6], the eddy current method [7], ultrasonic methods [8, 9], and X-ray methods [10]. These methods have some disadvantages, and it is impossible to achieve safe and efficient nondestructive testing (NDT) of the welded structure. To address this problem, shear horizontal- (SH-) guided wave detection methods have been proposed [2, 11–13]. Due to the low dispersion of the SH wave, the SH-guided wave in the weld seam can achieve long-distance weld inspection [14] and multiple defects can be detected from a single scan [15]. To identify multiple defect signals, one must study the propagation law of SH-guided waves in the weld seam.

SH-guided waves in the weld seam are usually studied by finite element methods [16–18]. In 1999, Spies [19] determined the radiation characteristics of an ultrasonic wave based on the description of SH-wave propagation in arbitrary-oriented transversely isotropic media. Slawinski and Krebes [20] later used a homogeneous approach to derive a finite difference scheme for modeling SH-wave propagation in fractured media. More recently, Yu et al. [11] studied high-order guided wave modes in the weld seam: modal analyses of an unbounded welded plate at high frequencies were conducted via a semi-analytical finite element approach. These studies show that there is dispersion when SH-guided waves propagate in the weld seam. Combined with the dispersion analysis of SH-guided waves in the plate, the dispersion equation of SH-guided waves in the weld seam can be obtained; however, the modeling results are quite different from experimental ones. To solve this problem, a nonlocal peridynamics method can be used to study the dispersion equation in the weld seam.

Silling [21] proposed the peridynamics theory in 2000 and studied the propagation and dispersion of linear

stress waves. Wave propagation in a discontinuity bar was studied two years later [22]. Zimmermann [23] explored many features of the peridynamics theory, including certain aspects of wave motion, material stability, and numerical solution techniques. The relationship between constitutive models from the classical theory of elasticity and peridynamics approach was reported by Silling et al. [24, 25]. Silling [25, 26] also developed a linearized version of the peridynamic theory applicable to small deformations. This theory offered simplifications that specialize the peridynamic equation and make it easier to solve.

Bažant et al. [27] systematically studied the peridynamics stress wave in 2016 and described wave dispersion behaviors in bond-based and state-based peridynamics. Butt et al. [28] focused on the dispersion properties of a state-based linear peridynamics solid model and specifically investigated the role of the peridynamics horizon in 2017. They investigated the effect of horizon size, mesh size, and the influence of weight function on the dispersion. In 2019, Zhang et al. [29] studied wave propagation and dispersion in the peridynamics medium and found that the SH wave also dispersed in an unbounded steel medium.

This study first introduces the basic theory of peridynamic waves and their reflection characteristics. The dispersion equation of the SH-guided wave in the weld seam is derived by analyzing the boundary condition of the SH-guided wave on the virtual layer. Combined with the SH wave in the infinite peridynamics medium that has dispersion characteristics [29], the wave group velocity varies with the wavenumber along the weld seam. Compared with the classical theory, the group velocity of the SH wave in the peridynamics medium is slightly slower than that from conventional theory. The influence of the difference in material parameters of the steel plate and the weld seam was analyzed as well as the existence of the weld residual height on the group velocity [30]. By compared the results obtained by the peridynamics theory with those from simulation and experiment, the peridynamics results are closer to the actual situation.

2. Peridynamic Theory

The linearized peridynamic theory has been proposed previously [21, 23, 25, 26]. The internal stress force of the linearized peridynamics theory is given as follows:

$$\sigma = \int_{N_x} C(x,q)\left(u(q,t) - u(x,t)\right)\mathrm{d}V_q. \tag{1}$$

Here, σ is the internal stress force, u is the displacement field, x is position in the reference configuration, and t is time. Term N_x is a neighborhood of x [9], and the radius of N_x is in general 2δ where δ is the radius of the horizon. Term q is the material point in N_x. C is a tensor-valued function called the "micromodulus function." When the SH-wave propagation is studied in a linear isotropic solid, the micromodulus C is defined as follows:

$$C(x,q) = \frac{15\mu}{\overline{m}^2}\int_{H_p} \varpi\left(|p-x|\right)\varpi\left(|p-q|\right)(p-x)\otimes(p-q)\mathrm{d}V_p. \tag{2}$$

Here, μ is the shear modulus, $\overline{m} = \int_H \omega(|\xi|)|\xi|^2\mathrm{d}V_\xi$ is the weighted volume, ϖ is the weighting function given by actual situation, and p is the material point in the horizon of x.

When given SH-wave propagating along the surface x_1ox_2, the direction of the shear force is x_3. The shear stress is written as follows:

$$\sigma_3 = \int_{N_x} c_{31}\left(u_1(q,t) - u_1(x,t)\right) + c_{32}\left(u_2(q,t) - u_2(x,t)\right) + c_{33}\left(u_3(q,t) - u_3(x,t)\right)\mathrm{d}V_q. \tag{3}$$

Since the SH wave has only displacement along the x_3 direction, (3) is reduced to

$$\sigma_3 = \int_{N_x} c_{33}\left(u_3(q,t) - u_3(x,t)\right)\mathrm{d}V_q. \tag{4}$$

Therefore, the SH wave is only affected by the micromodulus c_{33}. Since the weighted volume m and the bond in the integral term in formula (2) are only related to the geometric subdivision, the propagation of SH waves in different materials is only related to the shear modulus μ.

3. SH-Wave Dispersion in the Weld

To study the dispersion characteristics of the SH wave in the weld seam, the schematic of the SH-guided wave propagation in the weld seam is shown in Figure 1.

Figure 1 shows that o is the origin of the coordinates. The SH-guided wave in the weld seam propagates along the x_1; h is the thickness of the weld seam. There is a virtual boundary layer at the upper boundary of the weld seam; Δh is the mesh size and θ is the incidence angle of SH waves. Assume the wave equation of the SH-guided wave in the weld is

$$u(x_1,x_2,t) = A\exp\left[i\left(k_1x_1 + k_2x_2 + \omega t\right)\right]. \tag{5}$$

The weld seam has a free boundary, and the internal force at the virtual boundary layer is near to the boundary and is zero. To study the dispersion characteristics of the guide wave in the weld seam, a virtual material point x' is selected on the virtual boundary layer (Figure 1). From (1), the force at the material point on the virtual boundary is

$$\sigma = \int_{N_{x'}} C(x',q)\left(u(q,t) - u(x',t)\right)\mathrm{d}V_q = 0. \tag{6}$$

The horizon of the virtual material point x' is symmetrical relative to the normal x_2, and equation (6) can be written as follows (Figure 1):

$$\sigma = \int_{\mathrm{lef}\left(N_{x'}\right)} \left[C(x',q_0)\left(u(q_0,t) - u(x',t)\right) + C(x',q_2)\left(u(q_2,t) - u(x',t)\right)\right]\mathrm{d}V_q = 0. \tag{7}$$

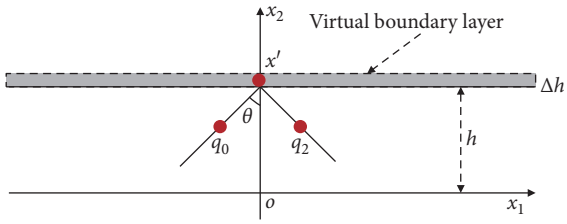

Figure 1: SH-guided wave in the weld seam.

Here, q_0 and q_2 are material points in the weld seam and are located symmetrically on both sides of the normal line (Figure 1). Term lef $(N_{x'})$ is the horizon on the left side of the normal, and the mesh is similar to the right horizon rig$(N_{x'})$. The two horizons are symmetrical about the normal. Therefore, the micromodulus at the two material points has the following features:

$$C(x', q_0) = C(x', q_2). \tag{8}$$

If there is a suitable horizon, then there are only two material points on the horizon due to the symmetry. The two material points fall on both sides of the normal, and equation (7) can be written as

$$\left(u\left(q_0^1, t\right) - u\left(x', t\right)\right) + \left(u\left(q_2^1, t\right) - u\left(x', t\right)\right) = 0. \tag{9}$$

The radius of the horizon is expanded so that the four material points fall into the horizon, leading to the following equation:

$$\left(u\left(q_0^2, t\right) - u\left(x', t\right)\right) + \left(u\left(q_2^2, t\right) - u\left(x', t\right)\right) = 0. \tag{10}$$

By analogy, for any two points in the horizon that are symmetric about the normal line, it can be written as follows:

$$\left(u\left(q_0, t\right) - u\left(x', t\right)\right) + \left(u\left(q_2, t\right) - u\left(x', t\right)\right) = 0. \tag{11}$$

After substituting (5) into (11) with rearrangement, it can be written as

$$\begin{aligned} &\exp\left[i\left(k_1\left(x_1^{p_0} - x_1'\right) + k_2\left(x_2^{p_0} - x_2'\right)\right)\right] - 1 \\ &\quad + \exp\left[i\left(k_1\left(x_1^{p_2} - x_1'\right) + k_2\left(x_2^{p_2} - x_2'\right)\right)\right] - 1 = 0. \end{aligned} \tag{12}$$

In Figure 1, assume the positional relationship of the material points in the weld seam upper surface as

$$\begin{aligned} x_1^{p_0} - x' &= -\Delta x_1, \\ x_2^{p_0} - x' &= -\Delta x_2. \end{aligned} \tag{13}$$

According to the symmetry of the two material points,

$$\begin{aligned} x_2^{p_2} - x_2' &= -\Delta x_2, \\ x_1^{p_2} - x_1' &= \Delta x_1. \end{aligned} \tag{14}$$

Substituting (13) and (14) into (11),

$$\exp\left[i\left(-k_1\Delta x_1 - k_2\Delta x_2\right)\right] + \exp\left[i\left(k_1\Delta x_1 - k_2\Delta x_2\right)\right] = 2. \tag{15}$$

Expanding the formula (15),

$$\cos\left(k_1\Delta x_1\right)\cos\left(k_2\Delta x_2\right) - i\cos\left(k_1\Delta x_1\right)\sin\left(k_2\Delta x_2\right) = 1. \tag{16}$$

When the boundary is the lower surface of the weld seam,

$$\cos\left(k_1\Delta x_1\right)\cos\left(k_2\Delta x_2\right) + i\cos\left(k_1\Delta x_1\right)\sin\left(k_2\Delta x_2\right) = 1. \tag{17}$$

Combining equations (16) and (17),

$$\cos\left(k_1\Delta x_1\right)\cos\left(k_2\Delta x_2\right) = 1, \tag{18}$$

$$\cos\left(k_1\Delta x_1\right)\sin\left(k_2\Delta x_2\right) = 0. \tag{19}$$

From equations (18) and (19),

$$\tan\left(k_2\Delta x_2\right) = 0. \tag{20}$$

Thus,

$$k_2\Delta x_2 = m_1\pi, \quad m_1 \in N^+. \tag{21}$$

From (11), it is known that the material point selection is arbitrary, and the thickness of the weld is h. Therefore, the conditions in equation (21) lead to the following equation:

$$k_2 h = m\pi, \quad m \in N^+. \tag{22}$$

Therefore, the dispersion equation of the guided wave of the weld can be obtained as follows:

$$\left(\frac{\omega}{c_T}\right)^2 - k_1^2 = \left(\frac{m\pi}{h}\right)^2. \tag{23}$$

Here, k_1 is the wavenumber of the weld direction, and c_T is a wave phase velocity in infinite media. The ratio of the group velocity in the weld c_g and phase velocity c_T in infinite media is as follows:

$$\frac{c_g}{c_T} = \frac{k_1}{\sqrt{(m\pi/h)^2 + k_1^2}}, \quad m \in N. \tag{24}$$

The wave velocity ratio of the SH-guided wave in the traditional theory [31] is as follows:

$$\frac{c_{g_0}}{c_{T_0}} = \frac{k_1}{\sqrt{(n\pi/h)^2 + k_1^2}}, \quad n \in N. \tag{25}$$

Here, c_{g_0} is the group velocity of the guided waves in the traditional theory, and c_{T_0} is the wave velocity in the infinite traditional theory. By comparing equations (24) and (25), the SH-guided wave has the same velocity ratio in the traditional theory and the peridynamics medium. Different modes of guided waves in the weld seam SH_m can be obtained when m is a different positive integer. When the weld has no weld residual height and the weld seam thickness is $h = 0.01$, the velocity ratio of the SH-guided wave in the weld seam can be shown in Figure 2.

Figure 2 shows that when the mode of the SH-guided wave in the weld seam is 0, the ratio of the velocity is always 1. When the mode of the guided wave increases, the wave

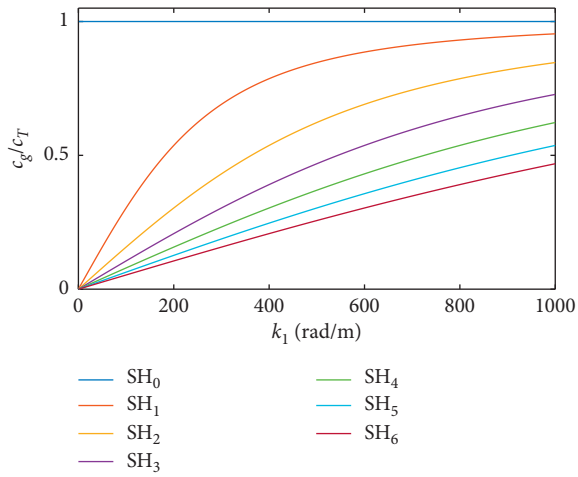

Figure 2: SH-guided wave velocity ratio in the weld seam.

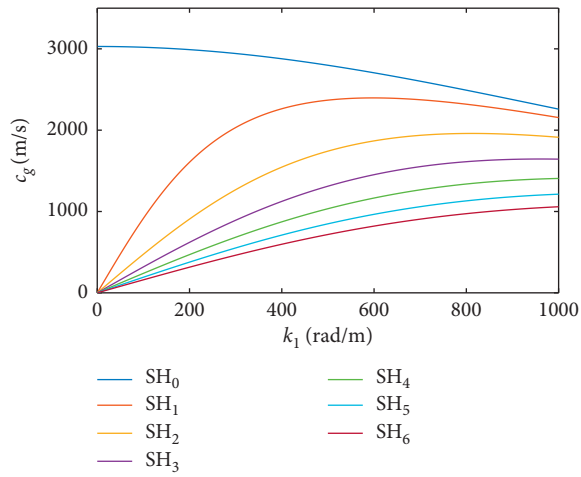

Figure 3: SH-guided wave group velocity of weld seam in the peridynamic medium.

velocity ratio gradually increases and eventually becomes 1. At the same wavenumber, a greater mode leads to a slower group velocity.

The dispersion equation of the SH-guided wave peridynamics medium is consistent with the traditional theory. However, the SH wave in the infinite peridynamics medium has dispersion characteristics, and the phase velocity of the SH wave that propagates in the peridynamics medium is slower than that of the traditional theory [31]. Therefore, the group velocity of SH-guided wave in the peridynamics medium is shown in Figure 3.

The group velocity of the SH$_0$-guided wave in the weld seam slows as the wavenumber increases due to the influence of the peridynamics method (Figure 3). These findings are consistent with the results of the experiment [32]. The group velocity of other guided wave modes increases with the wavenumber along the weld direction, but the rate of group velocity increase is slowed down under the influence of the peridynamics theory. The group velocity will decrease when the wavenumber reaches a certain value. Analysis of the SH$_1$ group velocity in Figure 2 shows that the group velocity of the SH-guided wave reaches a peak value of 2397 m/s when the wavenumber in the direction of the weld is about 594 rad/m. For a given wavenumber, a higher mode leads to a slower group velocity. The group velocity peak of the high mode appears at a higher wavenumber.

To analyze the relationship of guided waves in the weld seam between the peridynamic theory and traditional theory, SH-guided waves SH$_0$, SH$_3$, and SH$_6$ were studied in the peridynamics medium and compared to SH-guided waves SH$_0'$, SH$_3'$, and SH$_6'$ in the traditional theory. The group velocities are shown in Figure 4.

Figure 4 shows that the group velocity of the SH-guided wave in the peridynamics and traditional theory has similar trends with small wavenumber. The wave group velocity of SH$_0'$ is held at 3017 m/s. The SH wave in the infinite peridynamics medium has dispersion characteristics, and the group velocity of SH$_0$ decreases from 3029.2 m/s with an increase in the wavenumber. When the wavenumber is small, the group velocity of the SH-guided wave in the weld

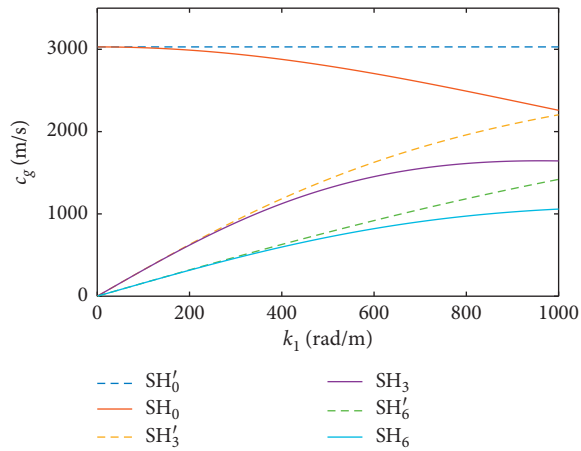

Figure 4: Comparison of the group velocity of SH-guided wave in peridynamics medium and traditional theory.

seam is greater but has an increasing wavenumber: the group velocity of the peridynamics experiment is lower than the traditional experiment. The dispersion of the SH wave is more obvious with increasing wavenumber, and the difference in the group velocity is obvious at higher wavenumbers. The group velocity of the other modes increases with wavenumber. In the case of the same mode, the group velocity in the peridynamics medium is lower than the traditional theory; the difference in the group velocity becomes larger as the wavenumber increases.

The group velocity of the SH-guided wave is different between the weld seam and the steel plate due to the differences in material parameters between the weld seam and the steel plate [13]. The wave equation in the traditional theory is a local differential theory, and there is a discontinuity of group velocities at the interface between the weld seam and the steel plate. This is inconsistent with the actual results. In the peridynamics theory, the group velocity of the SH-guided wave with slow transitions at the interface is due to the nonlocality of the peridynamics theory. This makes the group velocity at the interface closer to reality. The group

velocity of SH-guided waves SH_0 and SH_1 which are given by the numerical methods is shown in Figure 5.

Figure 5 shows the middle part of [−0.01, 0.01] in the weld seam; the other two sides are the steel plate. The group velocity of the SH-guided wave in the weld seam is lower than that in the steel plate because Young's modulus of the material in the weld seam is smaller than that in the steel plate. The group velocity of SH-guided waves at the interface has a slow downward trend, which is closer to reality than the cliff-type decline under the traditional theory [31]. This is a nonlocal characteristic of peridynamics.

Figure 5(a) shows that the group velocity of SH-guided waves decreases with increasing wavenumber, which coincides with the group velocity of the guided waves SH_0 in Figure 3. In NDT, the lower frequency is conducive to the excitation of a SH_0-guided wave. The waves number 100 rad/m is more appropriate. In Figure 5(b), the group velocity increases with increasing wavenumber. When the wavenumber surpasses 600 rad/m, the group velocity decreases, which is consistent with the group velocity of the weld-guided wave SH_1 (Figure 3).

There are two guided wave modes, SH_0 and SH_1, in NDT. Figure 5 shows that the group velocity of the two guided wave modes is approximately the same when the wavenumber is around 1000 rad/m. Thus, the two guided wave modes will be superposed. This is more suitable for the NDT of weld seams.

The factors affecting the group velocity of guided waves are not only the difference of materials but also the existence of the weld residual height during the welding process. This affects the thickness h of the weld seam. When there is a weld residual height in the weld seam, through the measurement of the weld seam, it is found that the change rule of h obeys equation (26):

$$h = \begin{cases} -12x^2 + 0.0106615, & |x| \le 0.01, \\ 0.01, & \text{else.} \end{cases} \tag{26}$$

Equation (24) suggests that the guided wave of the 0-order mode is not affected by the weld residual height, and the distribution of the group velocity is consistent with that in Figure 5(a). The SH-guided waves of other modes are affected by the weld residual height. The distribution of the group velocity of guided waves of SH_1 in the weld seam at different frequencies is shown in Figure 6.

In Figure 6, the dispersion of the SH-guided wave in the steel plate is consistent with that in Figure 5(b), and the dispersion characteristics remain unchanged in most areas. However, the group velocity decreases near the weld interface due to the difference in material parameters between the steel plate and the weld seam. The group velocity is also affected by the weld residual height in the weld seam. When the wavenumber along the weld is 200 rad/m, the group velocity increases gradually from both sides to the middle of the weld seam—this is consistent with the results obtained in the traditional theory [31]; When the wavenumber of the SH-guided wave is 400 rad/m and 600 rad/m, the group velocity first increases and then decreases. The group velocity increases until it reaches the maximum at the center of the weld seam. When the SH wavenumber is 800 rad/m, the group velocity first decreases and then increases; it reaches a peak at the center. By comparing the changes in the group velocity of the four wavenumbers, one sees that the group velocity is susceptible to the influence of the welding residual height at low wavenumbers. The influence of the weld residual height of the SH-guided wave group velocity decreases gradually with an increasing wavenumber along the weld direction. To improve the accuracy of testing in NDT, it is necessary to consider the welding height where the sensor is placed. This can precisely estimate the group velocity of the guided wave and thus precisely locate the defect.

4. Simulation and Experiment

A comparative analysis with the finite element simulation and experiment is needed to verify the correctness of the peridynamics theory. There are many modes of the SH-guided wave in the weld seam, which is not conducive to comparative analysis. Thus, the excitation of a single guided wave mode must be realized. Suppose that the super-generated wave function in the weld seam is

$$u(x_1, x_2, t) = \sum_{m=0}^{\infty} u_m(x_1, x_2, t). \tag{27}$$

Here, $u_m(x_1, x_2, t)$ is the single-mode weld SH-guided wave. Based on equation (5) of the SH-guided wave, we can obtain

$$u_m(x_1, x_2, t) = A_m \exp[i(k_{1m}x_1 + k_{2m}x_2 + \omega t)]. \tag{28}$$

Thus,

$$u(x_1, x_2, t) = \sum_{m=0}^{\infty} A_m \exp[i(k_{1m}x_1 + k_{2m}x_2 + \omega t)]. \tag{29}$$

Separating the time variable in the above equation can lead to the vibration form at the wave source:

$$u(0, x_2) = \sum_{m=0}^{\infty} A_m \exp(ik_{2m}x_2). \tag{30}$$

Equation (30) is a wave function and only has the real part. Its wavenumber k_{2m} is given by (22), and the above formula can be written as

$$u(0, x_2) = \sum_{m=0}^{\infty} A_m \cos\left(\frac{m\pi}{h}x_2\right). \tag{31}$$

From the Fourier series, the amplitude can be obtained as

$$A_m = \frac{2}{h}\int_0^h u(0, x_2, 0)\cos\left(\frac{\pi}{h}mx_2\right)d_{x_2}. \tag{32}$$

From the orthogonality of trigonometric functions, it concluded that

$$u(0, x_2) = \cos\left(\frac{\pi}{h}mx_2\right). \tag{33}$$

This is true only when $A_m \neq 0$. Therefore, at this time, ultrasonic waves excite only m modal weld-guided waves.

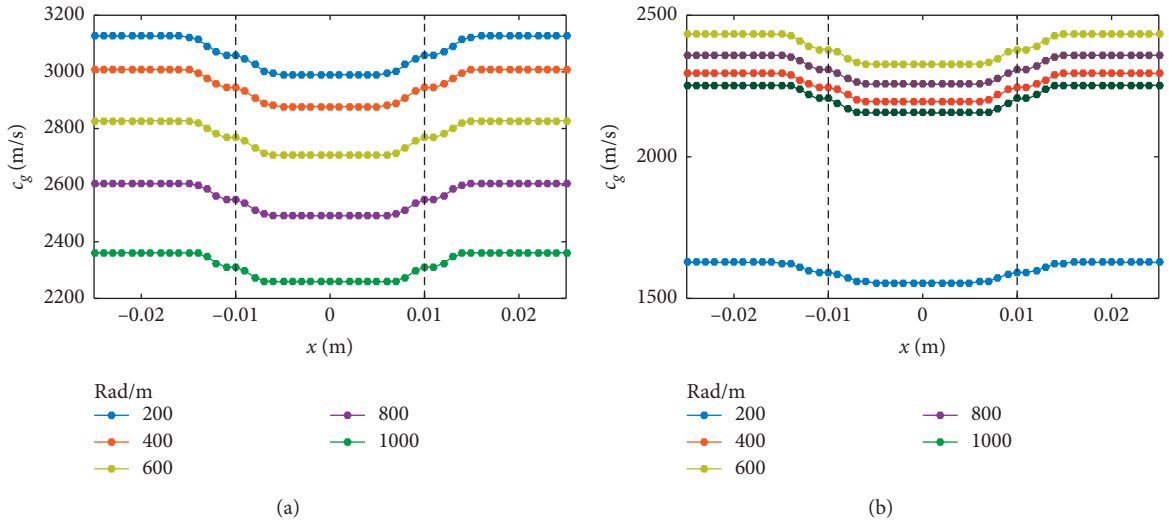

Figure 5: Distribution of the group velocity of guided waves with no weld residual height: (a) SH_0 and (b) SH_1.

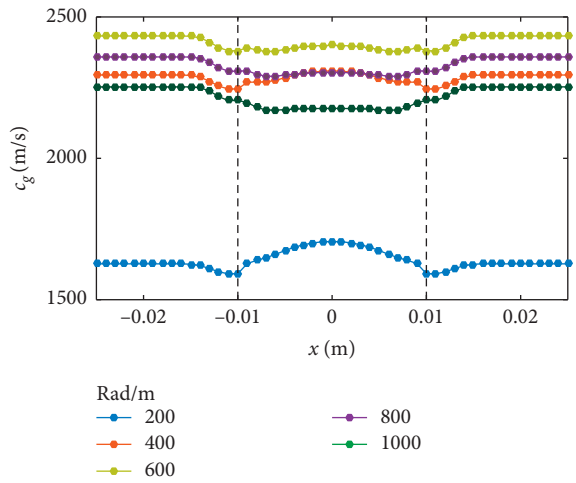

Figure 6: Distribution of group velocity of the guided wave SH_1 in weld seam under the influence of weld residual height.

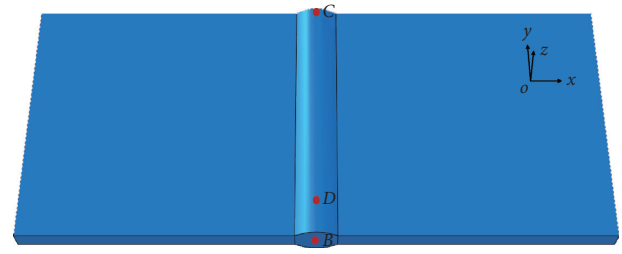

Figure 7: Schematic of the weld model.

At this point, the vibration law at the source can be obtained as

$$u(0, x_2, t) = \cos\left(\frac{\pi}{h} m x_2\right) \exp(i\omega t). \tag{34}$$

Therefore, a single-mode SH-guided wave can be excited when the load stress (34) is applied at one end of the weld seam.

To study the propagation characteristics of the SH-guided wave in the weld seam, the basic model is given as shown in Figure 7. Given two $600 \times 800 \times 10\ mm^3$ Q235b steel plates, the 600 mm weld seams are obtained by welding along the width direction according to a type II interface. The width of the weld seam is 20 mm, and the residual height of the weld seam is 0.33 mm. The direction perpendicular to the weld is the z-axis, and the direction along the weld is the x-axis. The thickness direction of the steel plate is the y-axis. The welded structure is shown in Figure 7.

Figure 7 shows that one end of the weld is B and the other end is C. The signal generator is placed at the cross-section of the weld seam at the B end. A signal receiver D is placed 30 mm away from the signal generator.

To study the propagation characteristics of the SH-guided wave in the weld seam, the weld seam material parameters are obtained by the tensile test. The material parameters of the weld seam and steel plates are shown in Table 1.

The excitation function of the guided wave is based on (34), and thus,

$$\tau(t) = A \cos\left(\frac{\pi}{h} m x_2\right) \exp(i\omega t). \tag{35}$$

Here, A is the amplitude of the modulated signal. In the finite element simulation, ABAQUS software is used to simulate the weld model in Figure 7 at a simulation mesh size of 0.5 mm. The element style is hexahedron, and there will be 800 element surfaces at the cross-section of the weld seam at the B end. The amplitude is 10 kPa when we give the load (35) at each surface. When selected a suitable m, the SH-guided wave will be excited. The signal receiver detects the shearing force along x_3 at point D. This experiment used an ultrasonic array to excite the SH-guided wave. According to equation (35), different loads are applied on different cells to excite the single-mode SH-guided waves in the weld seam; the amplitude is 10 V. Another sensor is placed at point D to collect the SH-guided wave signal through the oscilloscope. The signal in the finite element simulation and experiment is shown in Figure 8.

Table 1: Material parameters of the steel plate and the weld seam.

	Elastic modulus (GPa)	Poisson ratio	Density (kg/m^3)
Steel plate	210	0.30	7932
Weld seam	192	0.33	7900

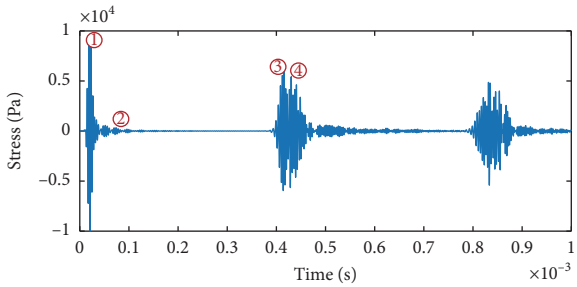

Figure 8: Sensor signal of SH-guided waves in the weld seam.

Figure 8 shows that the sensor first receives the vibration signal 1 from the top load at the B end. It subsequently receives signal 2, which is caused by wave dispersion. Signal 1 propagates to the C end and reflects forming signal 3. Signal 3 is reflected by B and is superimposed with the echo signal of signal 2 to form signal 4. The data analysis in Figure 8 shows that the peak value of signal 1 is 9368 Pa at 0.019 ms and signal 3 is 6035 Pa at 0.4157 ms. Combining the position of the sensor and the length of the weld, the group velocity of the SH-guided wave is 2949 m/s. The dispersion of the SH-guided wave in the weld seam can be concluded by the group velocity.

In experimental and finite element simulation, the SH-guided wave group velocity is obtained by detecting the wavenumber from $k_1 = 200$ rad/m along the weld length with intervals of 100 rad/m. A comparison of the SH-guided wave group velocity between simulation, experiment, and peridynamics is shown in Figure 9.

Figure 9 shows that the dispersion equation of the weld seam in the peridynamics medium can better reflect the group velocity of SH-guided waves with different modes than that of the finite element simulation. When the wavenumber along the welded direction is small, the results of peridynamics dispersion and finite element simulation are close, but there is a big gap between the experimental results. However, the gap between peridynamics and finite element simulation gradually increases with increasing wavenumber along the weld direction, but the error with experiment gradually decreases. The group velocity obtained by peridynamics is lower than that obtained by the finite element simulation because the SH wave in the infinite peridynamics medium has dispersion characteristics. The experimental results are much lower due to the interference in the actual experiment. When the wavenumber is higher, the energy of the guided wave is higher and is less affected by the outside. The given peridynamics parameters are not suitable for this situation, but the result of the group velocity in the experiment is higher than the peridynamics results. However, peridynamics can generally better reflect the group velocity

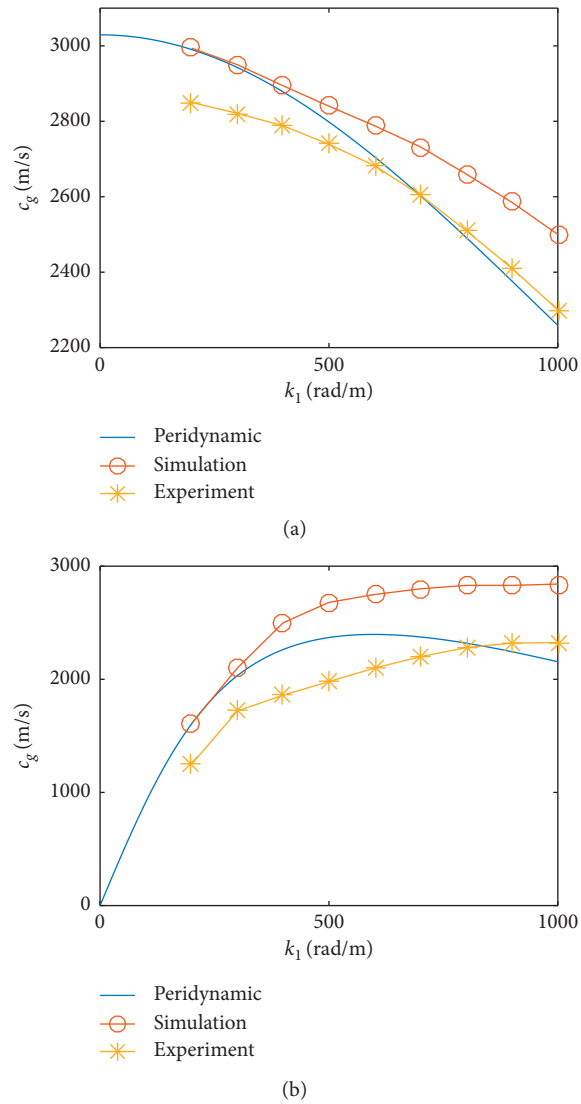

Figure 9: SH-guided wave group velocity in the weld seam (a) SH_0 and (b) SH_1.

characteristics of SH-guided waves in a weld seam with different modes.

To study the influence of material parameters and the weld residual height on group velocity distribution in the weld seam, a column of nodes in the weld structure was selected via finite element simulation. The group velocity at different nodes was obtained by processing the signals. In the experiment, 11 sensors were placed on a steel plate and weld seam to monitor the group velocity. Figure 10 compares the experimental and simulated group velocities measured by the sensor with the peridynamics results.

The wavenumber along the weld is 600 rad/m in Figure 10(a), the wavenumber is 200 rad/m in Figure 10(b). Figure 10 shows that the group velocity derived from the theory of peridynamics is basically between the simulation and experimental results. However, the results of peridynamics in Figure 10(a) are close to those from simulation due to the differences in the mode and the wavenumber of guided waves along the weld seam. The peridynamics results

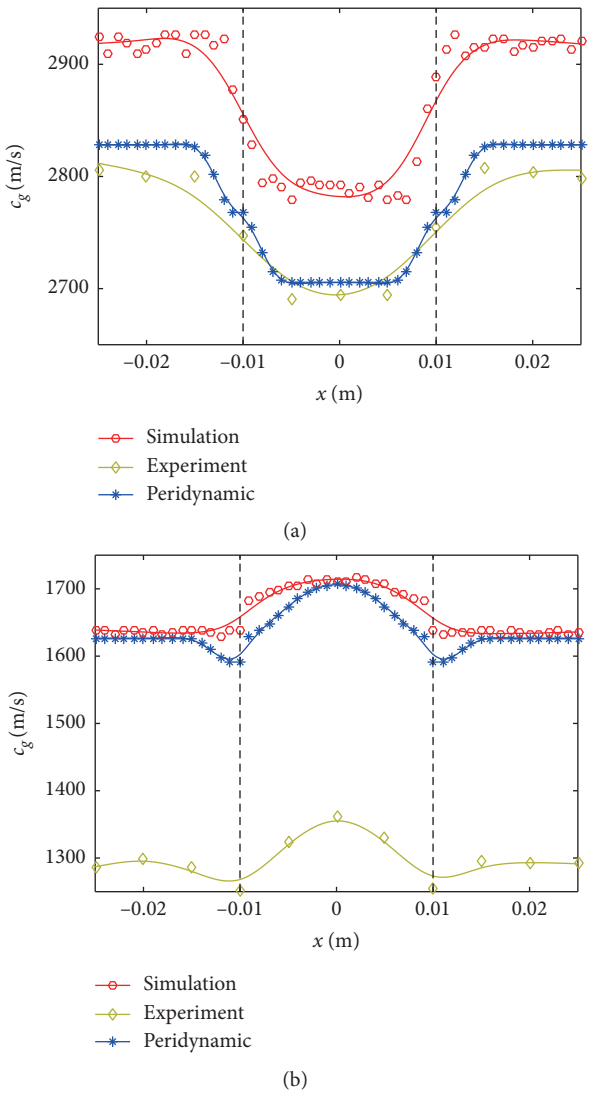

FIGURE 10: SH-guided wave group velocity distribution in the weld seam (a) SH_0 and (b) SH_1.

in Figure 10(b) are close to the simulation results. Figure 10(a) shows that the group velocity of the SH-guided wave decreases in the weld seam due to the difference in material parameters, but the group velocity decreases in the finite element are more obvious than those in peridynamics and experiments due to the local characteristics. In Figure 10(b), the group velocity in peridynamics and experiments has a significant decline at the welding interface, but this is not obvious in the simulation. Therefore, the SH group velocity distribution in the weld seam obtained from the peridynamics theory can better reflect the actual situation than the simulation. Therefore, the accuracy of defect location estimation can be improved via the group velocity simulations based on peridynamics in NDT.

5. Conclusions

In this study, the dispersion equation of SH-guided waves in weld seams is studied based on peridynamics. The dispersion equation of SH-guided waves in the weld seam based on the peridynamic medium is consistent with the traditional theory. However, the phase velocity in an infinite medium varies with the wavenumber due to the SH wave dispersion in the peridynamic medium. The group velocity of the SH-guided wave in the weld seam based on the peridynamic medium is smaller than that in the traditional theory. There is a difference in material parameters between the steel plate and the weld seam. Thus, the group velocity decreases slowly at the interface between the steel plate and the weld seam in peridynamics simulation. These values are closer to the actual situation than the discontinuous decline in the traditional theory. The group velocity increases as the weld residual height in the weld seam increases. These observations are consistent with the results of the traditional theory.

To verify the correctness of the peridynamic dispersion equation, the SH-guided wave of a single mode in the weld seam is excited by controlling the wave source in simulation and experiment; this leads to the group velocity of the SH-guided wave in simulation and experiment. By comparison, the group velocity of SH-guided waves in the weld seam based on the peridynamics theory is basically between the finite element simulation and the experiment results. The group velocity in the peridynamic medium is closer to the actual situation. This nicely reflects the SH-guided wave propagation characteristics in the weld structure. Therefore, the peridynamics theory can be widely used in NDT and can increase the precision of defect location.

Data Availability

The data used to support the findings of this study are available from the corresponding author upon request.

Conflicts of Interest

The authors declare that they have no conflicts of interest.

Acknowledgments

The work was supported by the National Natural Science Foundation of China (No. 51679112) and Postgraduate Research and Practice Innovation Program of Jiangsu Province KYCX17_1764. We thank LetPub (http://www.letpub.com) for its linguistic assistance during the preparation of this manuscript.

References

[1] J. L. Rose, Z. Sun, P. J. Mudge, and M. J. Avioli, "Guided wave flexural mode tuning and focusing for pipe testing," *Materials Evaluation*, vol. 61, 2003.

[2] Z. Fan and M. J. S. Lowe, "Interaction of weld-guided waves with defects," *NDT & E International*, vol. 47, pp. 124–133, 2012.

[3] B. Wu, Y. Cui, Y. Zhang, and C. He, "Propagation characteristics of Lamb wave and affected factors in butt welds," *College of Mechanical Engineering and Applied Electronics Technology*, vol. 22, pp. 818–829, 2014.

[4] Q. Huan and F. Li, "A baseline-free SH wave sparse array system for structural health monitoring," *Smart Materials and Structures*, vol. 28, no. 10, p. 105010, 2019.

[5] J. Tarraf, S. Mustapha, M. A. Fakih et al., "Application of ultrasonic waves towards the inspection of similar and dissimilar friction stir welded joints," *Journal of Materials Processing Technology*, vol. 255, pp. 570–583, 2018.

[6] G. S. Sodhi and J. Kaur, "Powder method for detecting latent fingerprints: a review," *Forensic Science International*, vol. 120, no. 3, pp. 172–176, 2001.

[7] C. P. Bean, R. W. DeBlois, and L. B. Nesbitt, "Eddy-current method for measuring the resistivity of metals," *Journal of Applied Physics*, vol. 30, no. 12, pp. 1976–1980, 1959.

[8] S. Halkjær, M. P. Sørensen, and W. D. Kristensen, "The propagation of ultrasound in an austenitic weld," *Ultrasonics*, vol. 38, pp. 256–261, 2000.

[9] M. A. Fakih, S. Mustapha, J. Tarraf, G. Ayoub, and R. Hamade, "Detection and assessment of flaws in friction stir welded joints using ultrasonic guided waves: experimental and finite element analysis," *Mechanical Systems and Signal Processing*, vol. 101, pp. 516–534, 2018.

[10] P. J. Webster, L. D. Oosterkamp, P. A. Browne et al., "Synchrotron X-ray residual strain scanning of a friction stir weld," *The Journal of Strain Analysis for Engineering Design*, vol. 36, no. 1, pp. 61–70, 2001.

[11] X. Yu, P. Zuo, J. Xiao, and Z. Fan, "Detection of damage in welded joints using high order feature guided ultrasonic waves," *Mechanical Systems and Signal Processing*, vol. 126, pp. 176–192, 2019.

[12] Z. Fan and M. J. Lowe, "Elastic waves guided by a welded joint in a plate," *Proceedings of the Royal Society A: Mathematical, Physical and Engineering Sciences*, vol. 465, no. 2107, pp. 2053–2068, 2009.

[13] Z. Fan, M. Castaings, M. J. S. Lowe, C. Biateau, and P. Fromme, "Feature-guided waves for monitoring adhesive shear modulus in bonded stiffeners," *NDT & E International*, vol. 54, pp. 96–102, 2013.

[14] A. Pau, D. Capecchi, and F. Vestroni, "Reciprocity principle for scattered fields from discontinuities in waveguides," *Ultrasonics*, vol. 55, pp. 85–91, 2015.

[15] D. V. Achillopoulou and A. Pau, "Characterization of defects in plates using shear and lamb waves," *Procedia Engineering*, vol. 199, pp. 2001–2007, 2017.

[16] Z. Xu and W. Chen, "Vibration analysis of plate with irregular cracks by differential quadrature finite element method," *Shock and Vibration*, vol. 2017, Article ID 2073453, 13 pages, 2017.

[17] M. Castaings and M. Lowe, "Finite element model for waves guided along solid systems of arbitrary section coupled to infinite solid media," *The Journal of the Acoustical Society of America*, vol. 123, no. 2, pp. 696–708, 2008.

[18] M. Cong, X. Wu, and R. Liu, "Dispersion analysis of guided waves in the finned tube using the semi-analytical finite element method," *Journal of Sound and Vibration*, vol. 401, pp. 114–126, 2017.

[19] M. Spies, "Computationally efficient SH-wave modeling in transversely isotropic media," *Journal of Nondestructive Evaluation*, vol. 19, no. 2, pp. 43–54, 2000.

[20] R. A. Slawinski and E. S. Krebes, "Finite-difference modeling of SH-wave propagation in nonwelded contact media," *Geophysics*, vol. 67, no. 5, pp. 1656–1663, 2002.

[21] S. A. Silling, "Reformulation of elasticity theory for discontinuities and long-range forces," *Journal of the Mechanics and Physics of Solids*, vol. 48, no. 1, pp. 175–209, 2000.

[22] S. A. Silling, M. Zimmermann, and R. Abeyaratne, "Deformation of a peridynamic bar," *Journal of Elasticity*, vol. 73, no. 1–3, pp. 173–190, 2003.

[23] M. Zimmermann, *A Continuum Theory with Long-Range Forces for Solids*, Massachusetts Institute of Technology, Cambridge, MA, USA, 2005.

[24] S. A. Silling, M. Epton, O. Weckner, J. Xu, and E. Askari, "Peridynamic states and constitutive modeling," *Journal of Elasticity*, vol. 88, no. 2, pp. 151–184, 2007.

[25] S. A. Silling and R. B. Lehoucq, "Peridynamic theory of solid mechanics," *Advances in Applied Mechanics*, vol. 44, pp. 73–168, 2010.

[26] S. A. Silling, "Linearized theory of peridynamic states," *Journal of Elasticity*, vol. 99, no. 1, pp. 85–111, 2010.

[27] Z. P. Bažant, W. Luo, V. T. Chau, and M. A. Bessa, "Wave dispersion and basic concepts of peridynamics compared to classical nonlocal damage models," *Journal of Applied Mechanics*, vol. 83, 2016.

[28] S. N. Butt, J. J. Timothy, and G. Meschke, "Wave dispersion and propagation in state-based peridynamics," *Computational Mechanics*, vol. 60, pp. 1–14, 2017.

[29] X. Zhang, Z. Xu, and Q. Yang, "Wave dispersion and propagation in linear peridynamic media," *Shock and Vibration*, vol. 2019, p. 9, 2019.

[30] X. Zhang and Z. Xu, "Formation mechanism of SH guided wave in weld seam," *Results in Physics*, vol. 16, p. 102840, 2020.

[31] J. L. Rose, *Ultrasonic Guided Waves in Solid Media*, Cambridge University Press, Cambridge, MA, USA, 2014.

[32] X. Zhang, Z. Xu, T. Yao, Y. Wang, and M. Wu, "The simulation of SH guided wave at weld by peridynamics theory," in *Proceedings of the 2019 IEEE Far East NDT New Technology and Application Forum (FENDT 2019)*, Institute of Electrical and Electronics Engineers Inc., Qingdao, China, June 2019.